X-RAYS OF STELLAR CORONAE WITH CHANDRA AND XMM-NEWTON

Flares and Elemental Composition in Stellar Atmospheres

Marc Audard[1]

Columbia Astrophysics Laboratory, Columbia University, Mail code 5247, 550 West 120th Street, New York, NY 10027, USA

Abstract

Observations of magnetically active stars with *Chandra* and *XMM-Newton* have deepened our knowledge of the physics of the atmospheres in late-type stars. In this review paper, I discuss two topics that have profited significantly from *Chandra* and *XMM-Newton*. Of particular interest, studies of the elemental composition of stellar coronae have taken advantage of the high spectral resolution available with the grating instruments on board these satellites. I summarize the status of our knowledge and discuss the elemental composition in a variety of stellar coronae. I also focus on the topic of flares in stellar coronae, and review the contributions made by *XMM-Newton* and *Chandra* to X-ray and multi-wavelength studies.

Key words: Stars: abundances – Stars: activity – Stars: atmospheres – Stars: coronae – Stars: flares – X-rays: stars

1. Introduction

X-ray astronomy of stars has been a rich and prosperous field for more than a quarter of a century (see reviews by Favata & Micela 2003; Güdel 2004). Late-type stars display strong X-ray emission as a signature of magnetic activity in their upper atmospheres (e.g., Linsky 1985). Stellar coronae have been studied in detail with many extreme ultraviolet (EUV) and X-ray satellites, but the launches of both *Chandra* and *XMM-Newton* finally gave access to high-resolution spectroscopy in the X-ray regime with high sensitivity. Of particular interest, the He-like triplets have given us access to electron densities which are of crucial importance to derive coronal volumes from emission measures (EMs). In addition, the elemental composition of the stellar coronal plasma can be obtained without much spectral confusion and the complication of radiative transfer for several abundant elements such as C, N, O, Ne, Mg, Si, S, Ar, Ca, and Fe.

Whereas the Sun's proximity helps to study the physical processes in its upper atmosphere, the investigation of X-ray coronae provides us with a wide range of physical conditions different from the Sun (e.g., mass, radius, rotation period, luminosity). The lack of spatial resolution in stars also helps us to obtain a global view of coronal physics in its most extreme conditions. Indeed, the solar corona does not sustain a corona with a dominant plasma temperature of a few tens of MK, but stars do.

This review summarizes the results obtained with the new *XMM-Newton* and *Chandra* X-ray satellites in the field of stellar coronae. About five years after their launches in 1999, there is a vast pool of publications and topics to review, too vast for merely 10 pages. Therefore, this review focuses on two specific topics, namely the elemental composition of stellar coronae (§2), and stellar flares (§3). Although I will address various issues related to abundances and flares, completeness is not possible given the limited space. I will therfore discuss selected representative examples in more detail but touch upon others only in a cursory way. A complementary review on the topics of densities and coronal structures can be found in these proceedings as well (Ness 2005). Previous reviews summarizing the view three years after the launch of *Chandra* and *XMM-Newton*can be found elsewhere (Audard 2003; Linsky 2003).

2. Elemental Composition of Stellar Coronae

2.1. A brief introduction

In the Sun, coronal abundances show a specific pattern in which elements with first ionization potentials (FIP) < 10 eV are enriched by a factor of ~ 4 with respect to their photospheric abundances. Although this so-called FIP effect can be observed in the full-disk emission of the Sun (Laming et al. 1995), details show, however, different FIP bias depending on where coronal abundances are measured (e.g., fast vs. slow wind, active regions, coronal holes, etc; see, e.g., Feldman & Laming 2000).

Coronal abundance studies in stars in the pre-*Chandra* and *XMM-Newton* era were promising but still in an infant state. Only the *EUVE* and *ASCA* satellites had sufficient spectral resolution to derive a few element abundances. The abundance of Fe in active stars was found to be deficient by factors of 5 to 10 relative to the solar photospheric abundance (e.g., S. Drake 1996; Schmitt et al. 1996). On the other hand, a solar-like FIP effect was derived in inactive stars (Drake et al. 1997; Laming & Drake 1999). The advent of *Chandra* and *XMM-Newton* have given further insight into the elemental composition in magnetically active stars thanks to their sensitive high-resolution grating spectra.

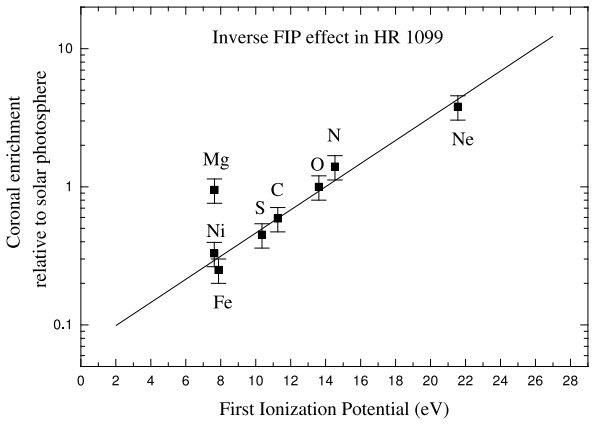

Figure 1. The inverse FIP effect as measured by Brinkman et al. (2001) in a deep XMM-Newton observation of HR 1099.

2.2. The FIP vs inverse FIP effects

A new pattern was observed in the active RS CVn binary system HR 1099 in which high-FIP (> 10 eV) elements are enhanced relative to the abundances of low-FIP elements (Fig. 1; Brinkman et al. 2001; Drake et al. 2001; Audard et al. 2001a). A detailed analysis of several active RS CVn binaries showed a similar inverse FIP effect (Fig. 2; Audard et al. 2003). Several studies with *Chandra* and *XMM-Newton* have confirmed the depletion of low-FIP elements (e.g., Fe), and the relative enhancement of high-FIP elements (e.g., noble gases Ar and Ne) in magnetically active stars (e.g., Güdel et al. 2001a; Güdel et al. 2001b; Huenemoerder et al. 2001; Gondoin et al. 2002; Raassen et al. 2002; Stelzer et al. 2002; Drake 2003; Gondoin 2003a; Gondoin 2003b; Huenemoerder et al. 2003; Osten et al. 2003a; Sanz-Forcada et al. 2003; van den Besselaar et al. 2003; Argiroffi et al. 2004; Audard et al. 2004; Gondoin 2004; Maggio et al. 2004; Schmitt & Ness 2004)

In solar analogs of different activity levels and ages, but of photospheric composition similar to the Sun's, the FIP bias is more complex: whereas young, active solar proxies showed an inverse FIP effect similar to that in the active RS CVn binaries, old, inactive stars show a solar-like FIP effect, suggesting a possible transition from one FIP pattern to the other with the level of activity (Güdel et al. 2002a; Telleschi et al. 2005). The lack of significant FIP bias in Capella (Audard et al. 2001b; Audard et al. 2003; Argiroffi et al. 2003), a wide RS CVn binary of interemediate activity, suggests that a transition in FIP bias occurs in this class of magnetically active stars as well. A solar-like FIP effect is also found in several giants (Scelsi et al. 2004; Garcia-Alvarez et al. 2005).

Although encouraging, the above general picture faces a significant challenge with Procyon. Whereas the cool, inactive coronae of α Cen AB both show solar-like FIP effects (Raassen et al. 2003a), no FIP bias is measured in the F-type subgiant (Raassen et al. 2002; Sanz-Forcada et al. 2004), consistently with *EUVE* (Drake et al. 1995). The FIP bias transition scenario, however, requires a strong solar-like FIP effect in cool, inactive stars.

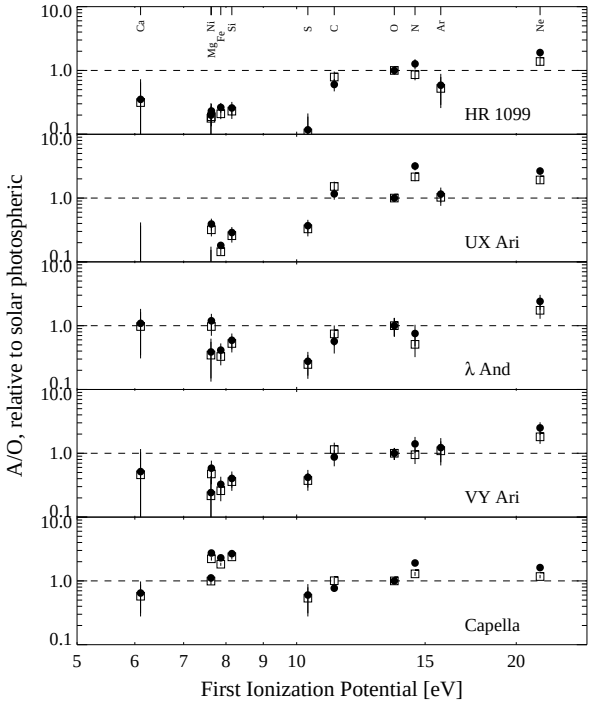

Figure 2. A systematic study of the coronal abundances in RS CVn binaries showed an inverse FIP effect in the most active stars, whereas the intermediately active Capella showed no specific bias (Audard et al. 2003). The symbols refer to different plasma emission codes.

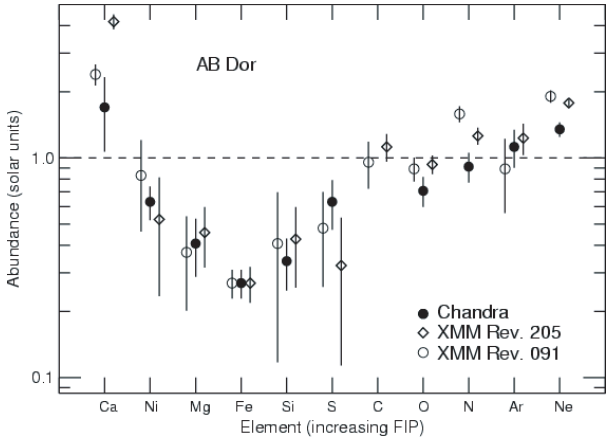

Figure 3. The coronal abundances in the fast rotating AB Dor. Notice the increase abundances at very low FIP (Ca and Ni; Sanz-Forcada et al. 2003).

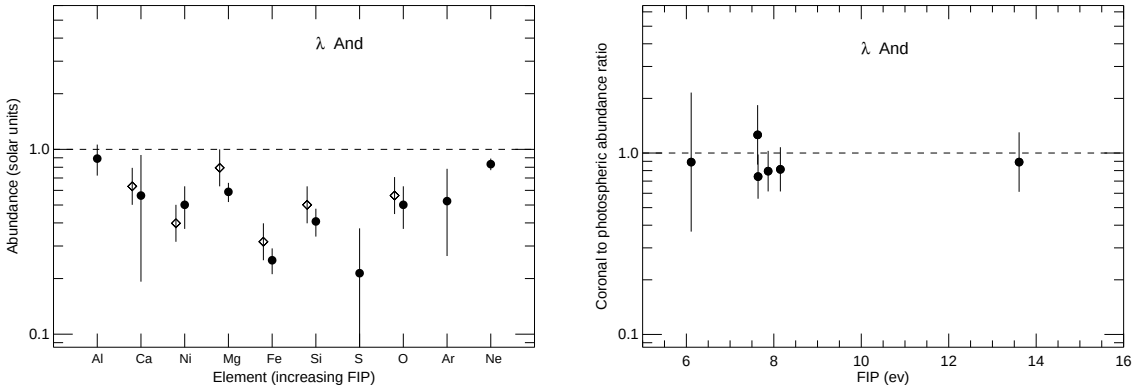

Figure 4. Coronal abundances in the RS CVn binary λ And. The U-shape pattern can be seen when the solar photospheric set is used as comparison (Left). On the other hand, no FIP bias is visible when stellar photospheric abundances are used (adapted from Sanz-Forcada et al. 2004; see also Audard et al. 2003).

Furthermore, several studies have reported that, whereas coronal abundances decrease with decreasing FIP in active stars, a turnover occurs at very low FIP where the abundances of the respective elements steeply increase (Fig. 3; Sanz-Forcada et al. 2003; Osten et al. 2003a; Huenemoerder et al. 2003; Argiroffi et al. 2004). The explanation for such a turnover remains unclear, as different analysis techniques provide different results for the same data sets (e.g., Argiroffi et al. 2004; Telleschi et al. 2005). It is worthwhile to mention that, in the Sun's corona, the abundances of elements at very low FIP are often larger than that of the low-FIP (Fe, Mg, Si) elements (see Feldman & Laming 2000 for a discussion).

An important caveat needs, however, to be raised: most studies rely on the solar photospheric abundances as the standard comparison set (e.g., Anders & Grevesse 1989; Grevesse & Sauval 1998). But the derivation of stellar photospheric abundances in magnetically active stars is challenging as such stars rotate fast, thus the signal-to-noise ratio of lines against the continuum is significantly reduced. In addition, spots and plages can distort the line shapes as the star rotates. Consequently, photospheric abundances can be highly uncertain, with major differences found in the literature, or, as is often the case, they are not available altogether (except perhaps the metallicity [Fe/H]).

The FIP coronal pattern could be different when real photospheric values for the individual stars are taken into account (Fig. 4; Audard et al. 2003; Sanz-Forcada et al. 2004). However, since the solar analogs sample used by Güdel et al. (2002a) and Telleschi et al. (2005) have photospheric compositions which are believed to be similar to the Sun's, the finding of a transition from inverse FIP to solar-like FIP effect with decreasing activity level appears to be robust. Also, several stars with known Fe photospheric abundances show a marked Fe depletion in the corona (e.g., Huenemoerder et al. 2003; Audard et al. 2004), suggesting that the inverse FIP effect is real.

Finally, the ill-posed problem of spectral inversion needs to be recalled in this review. Craig & Brown (1976a) and Craig & Brown (1976b) showed that statistical uncertainties can introduce significant uncertainty in the reconstructed emission measure distribution. In addition, systematic uncertainties introduced by, e.g., inaccurate calibration or incorrect atomic parameters in databases can increase the scatter further. Consequently, the effects on the derivation of coronal abundances can be severe unless external assumptions are introduced. Future studies need to take into account this basic problem, and to compare the output with different analysis techniques and atomic databases (e.g., Audard et al. 2004; Schmitt & Ness 2004; Telleschi et al. 2005).

2.2.1. The models

Models that aim at explaining the solar FIP effect are plenty (see the reviews by Hénoux 1995; Hénoux 1998; see also Arge et al. 1998; Schwadron et al. 1999; McKenzie 2000). On the other hand, the recent *Chandra* and *XMM-Newton* results still lack theoretical explanations. Güdel et al. (2002a) suggested that the non-thermal electrons seen in magnetically active stars could explain the inverse FIP effect, and possibly the FIP effect observed in inactive stars. Although promising, the scenario still remains in an infant state. To my knowledge, the model by Laming (2004) is the only comprehensive theoretical model that specifically addresses the inverse FIP effect in stars. The model proposes a unified picture of both the FIP and inverse FIP effects by exploring the effects on the upper chromospheric plasma of the wave ponderomotive forces. Laming (2004) suggested that fine tuning of the model parameters could turn a solar FIP effect into an inverse

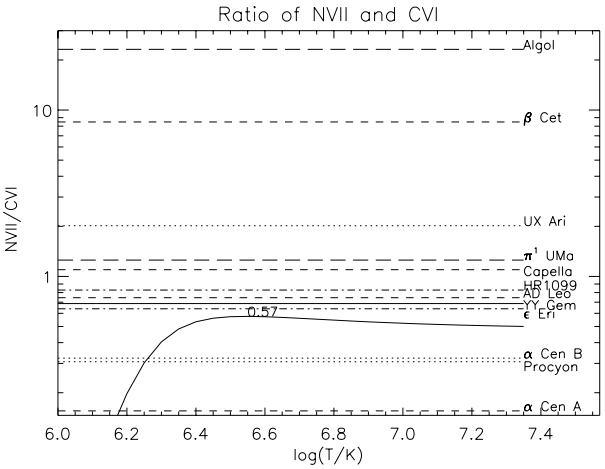

Figure 5. Line ratios of N VII *and* C VI *shown with the theoretical line ratio for solar photospheric abundances and the MEKAL atomic database as a function of the plasma temperature. The line ratios in Algol and β Cet lie significantly above the solar ratio, indicating the presence of CNO-cycle processed material at the stellar surface (Schmitt & Ness 2002).*

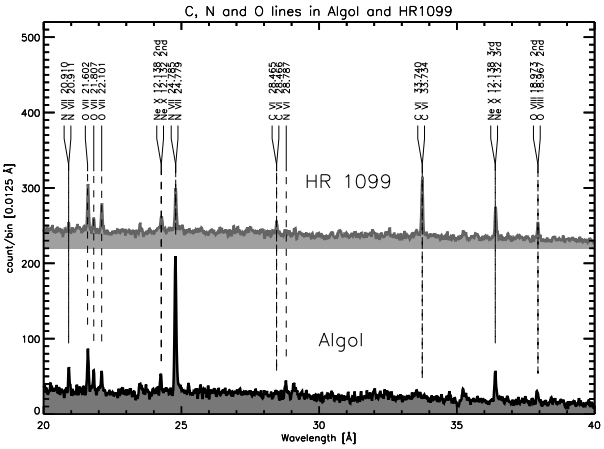

Figure 6. Extracts of the LETGS spectra of HR 1099 (top) and Algol (bottom). Notice the enhanced N VII Lyα *line at* 24.7 *Å and the faint* N VII Lyα *line in Algol, whereas the situation is almost reversed in HR 1099 (Drake 2003).*

FIP effect. Further theoretical works are needed to assess the validity of the proposed model, and to develop new models and ideas. The work in stellar coronae can thus provide important ideas and constraints on the solar element fractionation models.

2.3. Signatures of the CNO cycle

Whereas most stars show coronal abundances affected by element fractionation in their upper atmospheres, a few stars have shown enhanced N emission lines compared to what could be expected by, say, an inverse FIP effect. In particular, the N VII/C VI line ratio, which is about constant for temperatures of above 2.5 MK, turns out to be significantly non-solar in several stars (Fig. 5). Such high line ratios were interpreted as a signature of the CNO-cycle processed material (Schmitt & Ness 2002). Using the N/C abundance ratio as a diagnostic tool, Drake (2003) showed that the secondary star in Algol must have lost at least half of its initial mass onto the primary through accretion (Fig. 6). Evidence of the CNO cycle has also been found in the Algol-type RZ Cas (Audard et al. 2005). Some giant stars show evidence for CNO-processed material at their surface as well (β Cet: Schmitt & Ness 2002; YY Men: Audard et al. 2004). Finally, Drake & Sarna (2003) measured a strong [C/N] depletion in the pre-cataclysmic binary V471 Tau which they interpreted as observational evidence of the common envelope phase of the system.

2.4. Abundance variations during stellar flares

In the chromospheric evaporation model, fresh material is brought up from the chromosphere into the corona after electron beams impact and heat up the lower parts of the atmosphere (Antonucci et al. 1984). Therefore, X-ray spectra are expected to reflect abundances closer to the photospheric (actually chromospheric) composition. The increase of the average metallicity, Z, has been measured in several stellar flares with previous missions. *ASCA* measured in a flare in UX Ari a selective increase of low-FIP elements whereas high-FIP element abundances stayed nearly constant (Güdel et al. 1999; Osten et al. 2000). A similar behavior was observed with gratings in other stars (Audard et al. 2001a; Raassen et al. 2003b). However, this picture is not unique: other flare spectra displayed no

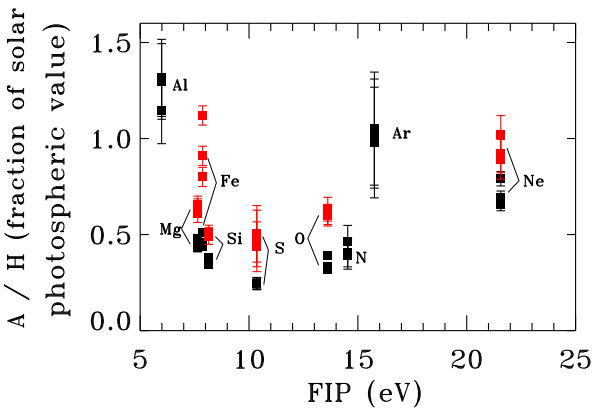

Figure 7. Coronal abundances in σ^2 CrB. During a stellar flare, all element abundances increase, with no specific FIP-related bias (Osten et al. 2003a).

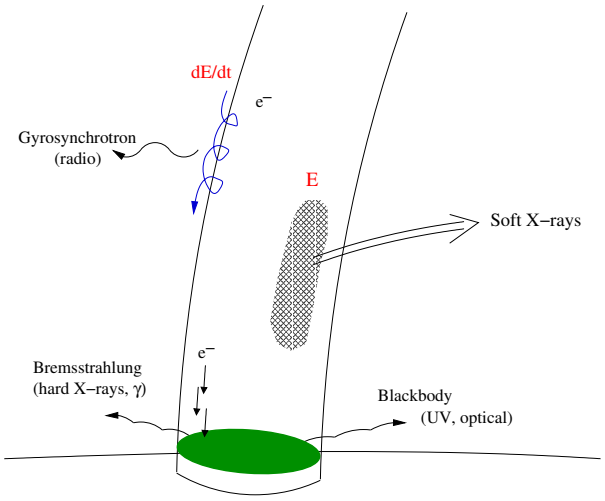

Figure 8. Sketch of the chromospheric evaporation model and the Neupert effect (Neupert 1968; see text for details).

FIP-related bias, i.e., all element abundances increased (Fig. 7; Osten et al. 2003a; Güdel et al. 2004). In addition, some flares show no evidence of abundance increase at all (Huenemoerder et al. 2001; van den Besselaar et al. 2003). In conclusion, the abundance behavior during flares remains unclear, possibly due to the low signal-to-noise ratios of time-dependent flare spectra.

3. Stellar Flares

Magnetically active stars have been known to display numerous flares in general (with the exception of a few notable examples, e.g., Capella and Procyon). Such flares can show extreme X-ray luminosities (up to a few percents of the stellar bolometric luminosity), very hot temperatures of more than 10 MK, and can last from minutes up to several days. In addition, flares can bring "fresh" chromospheric material up into the corona (Antonucci et al. 1984). Recent works also suggest that flares can act efficiently as stochastic agents to heat the corona in the Sun (Parker 1988) and in stars (Güdel 1997; Audard et al. 2000; Kashyap et al. 2002; Güdel et al. 2003a; Arzner & Güdel 2004). *Chandra* and *XMM-Newton* have observed several flares in magnetically active stars, including rather bright events. I summarize below the results obtained with those satellites and in multi-wavelength campaigns.

3.1. The Neupert Effect

The Neupert effect (Neupert 1968) describes the correlation between the microwave/radio light curve of flares and their X-ray light curve. The latter follows relatively closely the time integral of the former, and this effect has been explained in the context of chromospheric evaporation (Fig. 8; Antonucci et al. 1984; Fisher et al. 1985).

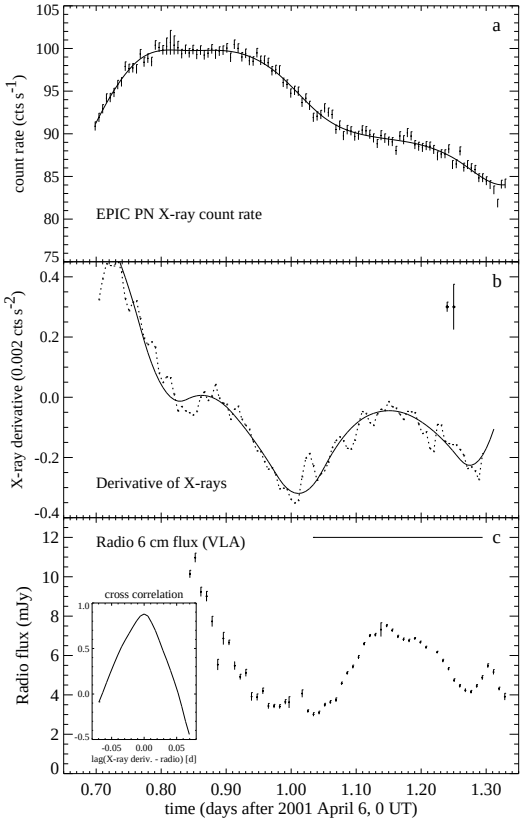

Figure 9. Evidence for the Neupert effect in the RS CVn σ Gem. Shown are the light curves observed in X-rays (top), its X-ray derivative (middle), and in radio (bottom). The inset shows a cross-correlation function between the X-ray derivative and radio light curves (Güdel et al. 2002b).

A beam of non-thermal electrons is accelerated from the magnetic reconnection site. Part of the electron beam gets trapped in the magnetic flux tubes and radiate gyrosynchrotron emission in the radio, and part of it impacts on the dense chromosphere producing hard X-ray non-thermal bremsstrahlung (and almost simultaneously broadband optical light). The beam heats up the upper chromosphere to coronal temperatures; the plasma in turn expands into coronal loops and subsequently cools radiatively in X-rays. The X-ray emission roughly scales with the thermal energy content deposited by the electron beam, whereas the radio/hard X-ray/optical emission relates to the energy rate (since these emissions are spontaneous, i.e., the radiative time scales are much shorter than in the X-rays).

Evidence of the Neupert effect has been found in the RS CVn binary σ Gem (Fig. 9; Güdel et al. 2002b). Whereas the VLA radio and *XMM-Newton* pn X-ray light curves show no apparent correlation, the derivative of the X-ray

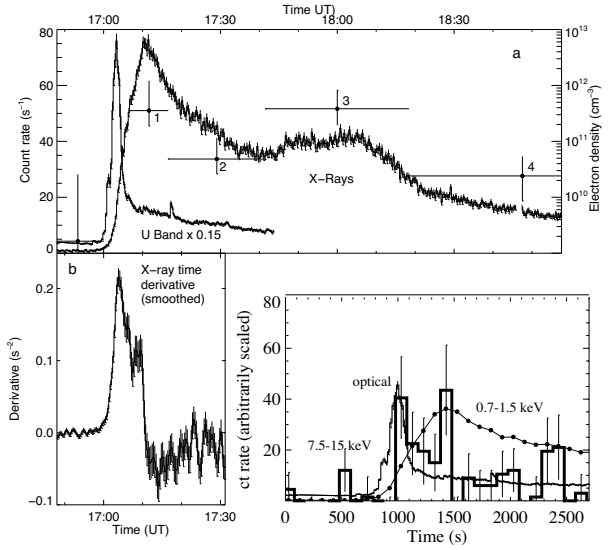

Figure 10. The Neupert effect in Proxima Centauri. The X-ray and optical light curves are shown in the top panel; the X-ray derivative is shown in the bottom left panel, whereas the hard X-ray ($7.5-15$ keV) light curve is shown as a histogram in the bottom right panel (adapted from Güdel et al. 2002c).

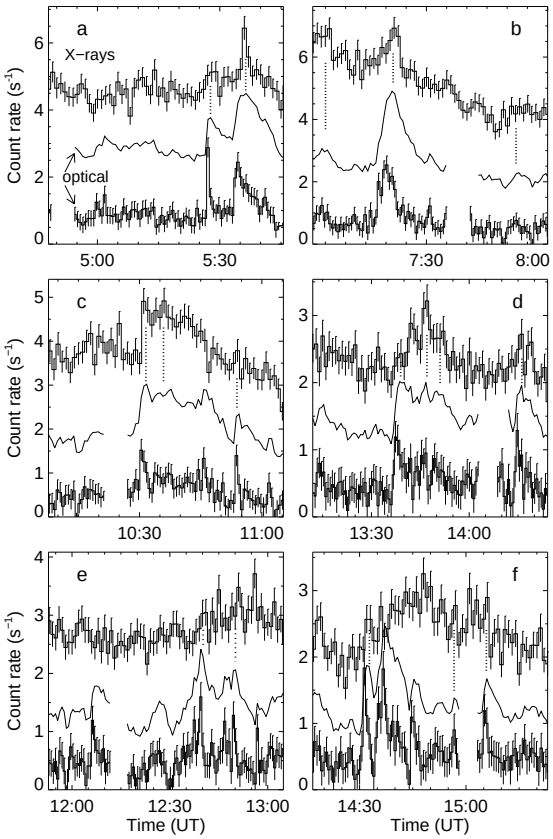

Figure 11. Several small flares are detected in the pseudo-"quiescent" X-ray and optical light curves of Prox Cen. Some also display a Neupert effect (Güdel et al. 2002c).

light curve follows closely the radio, as expected from the Neupert effect. A rough assessement of the flare energy budget showed that the energy in the non-thermal electrons is probably sufficient to heat the observed plasma. Indeed, under realistic assumptions, Güdel et al. (2002b) obtained an injected energy $E \sim 10^{33-36}$ ergs, similar to the X-ray emitted $E_{\rm X} \sim 4 \times 10^{34}$ ergs. In a systematic study of the X-ray and radio simultaneous observations of several M-type flare stars, Smith et al. (2005) also observed several cases of a Neupert effects, although they reported events where no radio counterparts were observed to X-ray flares, and vice-versa. They argued that, like in the Sun, not all flares should display a Neupert effect since the observable fluxes can originate from different mechanisms (e.g., radio masers) or spatial structures.

A large flare in Proxima Centauri was caught with *XMM-Newton*. Simultaneous coverage with the Optical Monitor proved helpful to observe the Neupert effect (Güdel et al. 2002c). In analogy with σ Gem, the X-ray derivative light curve closely matched the optical U-band light curve. X-ray photons in the range $7.5-15$ keV also occurred in the early phase of the flare (Fig. 10). The peak flare X-ray luminosity reached 3.9×10^{28} erg s^{-1}, about hundred times the pre-flare level (6×10^{26} erg s^{-1}), and the total energy radiated in X-rays was about 1.5×10^{32} ergs. There was spectroscopic evidence of density variations from $< 2 \times 10^{10}$ cm^{-3} (pre-flare) to 10^{11-12} cm^{-3} at flare peak. Together with the EMs, coronal volumes and masses could be derived as well. Reale et al. (2004) analyzed the Prox Cen flare with hydrodynamical codes and found that it could be described by an initial flare heating in a single loop ($\sim 10^{10}$ cm) followed by additional heating in an arcade-like structure. Güdel et al. (2004) found a similar loop size from a 2-ribbon flare modeling.

Further evidence of the Neupert effect and chromospheric evaporation was detected in the pre-flare light curve in Prox Cen, before the giant flare. The "quiescent" light curve turned out to be quite variable: a multitude of small events were detected in the X-ray *and* optical light curves, with the smallest events having X-ray luminosities $L_{\rm X} \sim 10^{26}$ erg s^{-1}, i.e., similar to modest solar flares (Güdel et al. 2002c). Many of them showed a Neupert effect, but some did not which is no different than in the Sun (Dennis & Zarro 1993). Such observations demonstrate that what is perceived as quiescence could in fact be explained by the superposition of a multitude of small heating flares.

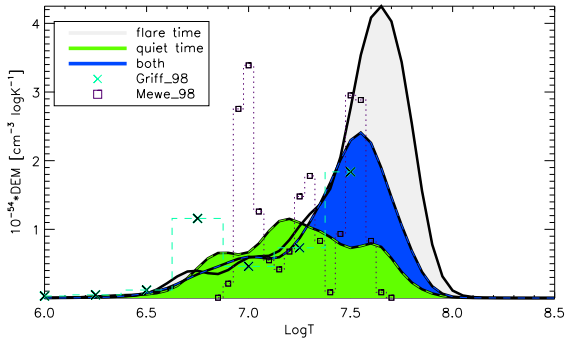

Figure 12. The EMD of the RS CVn binary II Peg (Huenemoerder et al. 2001). The time-averaged EMD is a composite of the "quiescent" EMD and the flare EMD.

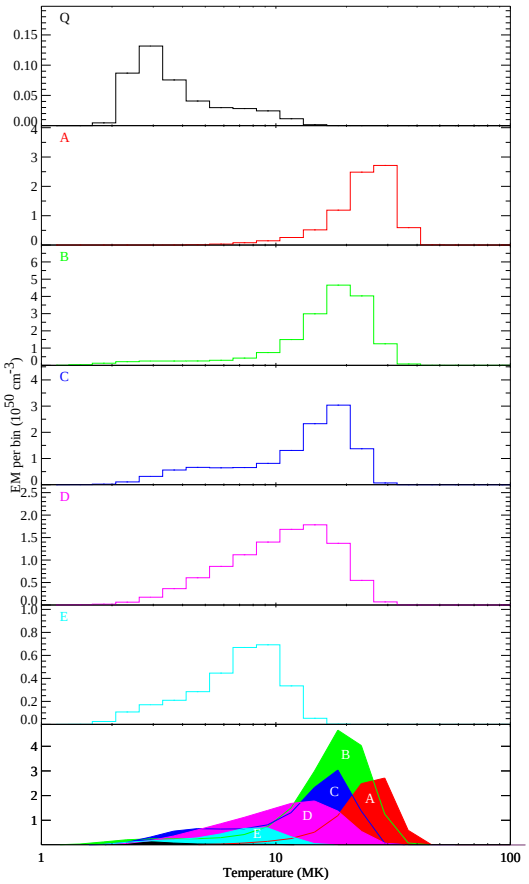

Figure 13. EMDs of Prox Cen (Güdel et al. 2004). The "quiescent" EMD is shown at the top, whereas the time-dependent flare EMD is shown in the subsequent panels. The bottom panel shows a superposition of all EMDs on the same vertical scale.

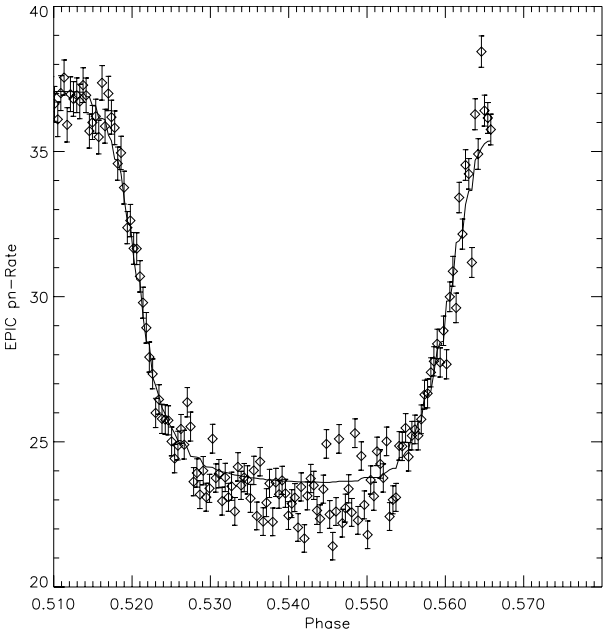

Figure 14. The XMM-Newton X-ray light curve of an eclipsed flare in Algol after correction using a flare decay profile (Schmitt et al. 2003). The best-fit model is shown as a solid curve. Fig. 15 shows the reconstructed spatial image.

3.2. The Flare Emission Measure Distribution

Flare spectra have displayed spectroscopic characteristics of high temperatures, such as a well-developed bremsstrahlung continuum and emission lines of highly ionized Fe (e.g., Audard et al. 2001a; Osten et al. 2003a). The reconstructed emission measure distribution (EMD) during flares indeed show strong EMs at high temperatures (Fig. 12; Huenemoerder et al. 2001; Raassen et al. 2003b; van den Besselaar et al. 2003). Time-dependent analyses actually revealed that the flare EMD evolves from a dominant high temperature in the early phase followed by a gradual decrease in emission measure and temperature (Fig. 13; Güdel et al. 2004).

Although the EMD temporarily evolves to high temperatures and returns to a pre-flare shape, the question arises whether flares as a statistical ensemble (i.e., from small to large flares) can shape the EMD of stellar coronae (e.g., Güdel 1997; Güdel et al. 2003a). In this framework, Güdel et al. (2004) noted that the large flare in the modesty X-ray active Prox Cen was equivalent to a small "wiggle" in the extremely X-ray active flare star YY Gem and further emphasized that the flare spectrum of Prox Cen closely matched YY Gem's *quiescent* spectrum. Audard et al. (2004) also showed that the high-temperature tail of YY Men's EMD can be ascribed to numerous small flares despite the lack of obvious flares in its light curve.

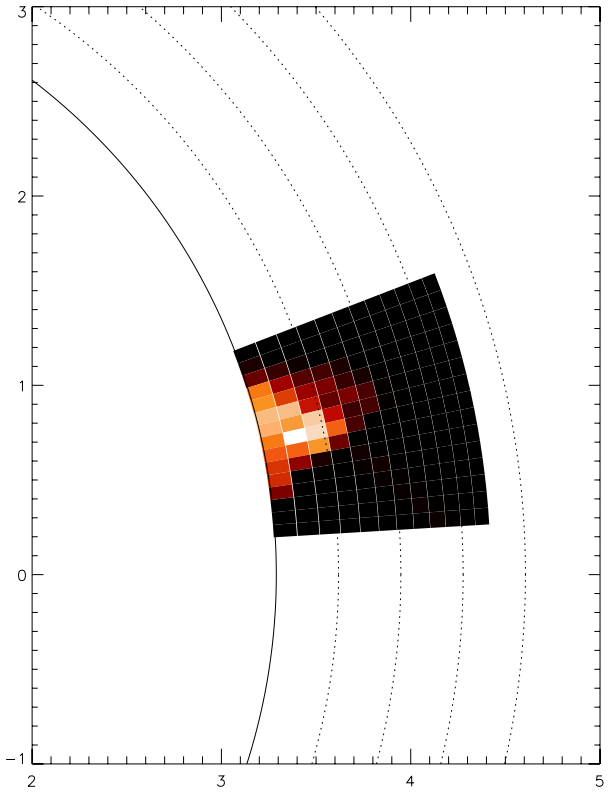

Figure 15. The reconstructed spatial image of the flare in Algol (see Fig. 14). The solid curve describes the photosphere of the K-type secondary, whereas the dotted curves denote successive heights in units of $0.1R_\star$ *(Schmitt et al. 2003).*

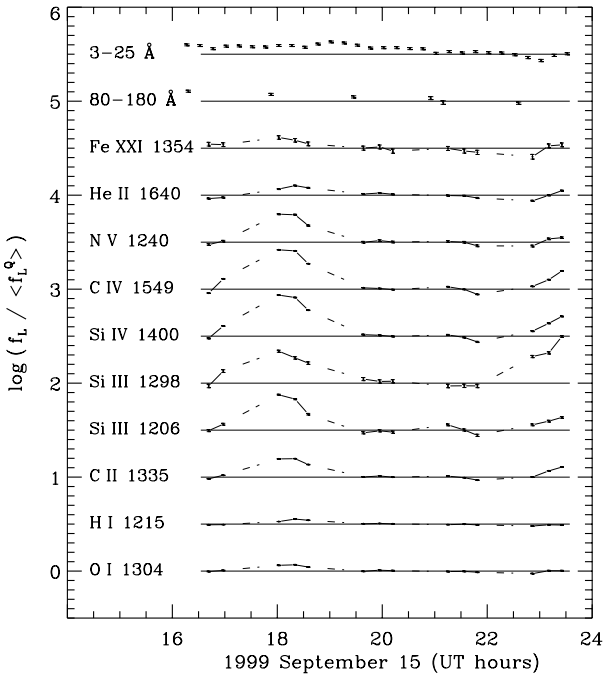

Figure 16. Light curves in X-rays, EUV, and in several UV emission lines (Ayres et al. 2001). The first top three curves are sensitive to hot (> 0.1 MK) plasma. Notice that the UV "cool" flares are not detected in those curves.

3.3. Eclipse Mapping

Schmitt et al. (2003) observed in Algol an eclipse of a flare that was in progress. Assuming a flare decay profile, they modeled a rectified light curve with an eclipse mapping code to derive the properties of the eclipsed flare. Schmitt et al. (2003) constrained the location of the flare to near the limb of the magnetically active K2 star at a height of $\sim 0.1R_\star$. The cumulative density distribution indicates densities of at least 10^{11} cm^{-3} and up to $\sim 2\times10^{11}$ cm^{-3}. Similar densities are derived from spectroscopy (O VII He-like triplet). A similar eclipsed flare was observed with *Beppo*SAX (Schmitt & Favata 1999; Favata & Schmitt 1999).

Eclipse mapping is a powerful means to obtain indirect information on the spatial structure of stellar coronae. Güdel et al. (2001b), Güdel et al. (2003b), and Güdel et al. (2005) used a similar method to obtain spatial maps of the eclipsing binaries YY Gem, α CrB, and CM Dra. Inhomogeneous coronal maps were derived, albeit with characteristics different from the Sun's (e.g., high altitudes). Audard et al. (2005) observed the eclipsing Algol-type RZ Cas with *XMM-Newton* and the VLA. Only shallow eclipses were detected with a different timing in the different wavelength regimes, suggesting extended emitting sources. Another technique to derive spatial information includes spectroscopy. Ayres et al. (2001) monitored the centroid of the Ne X Lyα line in HR 1099 over half an orbital period and concluded that the bulk of the X-ray emission was confined to the K-type secondary. Brickhouse et al. (2001) observed line centroid shifts in the contact binary 44i Boo. They found that derived that two active regions on the primary star at high latitudes could reproduce the observed line profile shifts and the X-ray light curve. YY Gem showed variable line broadening (Güdel et al. 2001b), whereas line shifts were measured in Algol (Chung et al. 2004).

3.4. Cool flares

Common wisdom assumes that flares show typically extreme high temperatures. However, Ayres et al. (2001) observed "cool" flares in a multi-wavelength campaign on HR 1099. The flares displayed temperatures less than 0.1 MK since there was no signal detected in the X-ray or EUV regimes, neither in the Fe XXI coronal line at λ1354 Å (Fig. 16). Such cool flares were interpreted as similar to transition zone explosive events observed in the Sun (Dere et al. 1989). Osten et al. (2003b) also reported a flare in radio/optical with no X-ray counterpart in EV Lac.

4. Concluding Remarks

The previous pages have provided a glimpse of the exciting new results in stellar coronal physics obtained with *XMM-Newton* and *Chandra* to date. The wealth of scientific publications five years after the satellites' launches is a lively proof of rapid advances in our field. I have concentrated on selected aspects, i.e., the elemental composition and stellar flares. Further topics are covered in a companion review in these proceedings (Ness 2005). Furthermore, numerous poster papers in these proceedings complement the present review as well. The field of stellar coronae has matured and profited significantly from *XMM-Newton* and *Chandra*. Nevertheless, future studies are needed to deepen our knowledge on stellar coronae in X-rays and at other wavelengths, and in particular to understand the connection between the Sun and magnetically active stars.

Acknowledgements

This review is dedicated to the late Dr. Rolf Mewe whom I met while a graduate student, and who left us too early. His knowledge, his kindness, and his friendship will be greatly missed.

I would like to thank the SOC of the CS13 workshop for their invitation to present this review. I also acknowledge fruitful discussions with his colleagues over the past few years in this research field. I am grateful to Manuel Güdel and Rachel Osten for their useful suggestions to improve this review. Rachel Osten, Dave Huenemoerder, and Jeremy Drake are also thanked for providing electronic versions of figures. Finally, the respective authors, the American Astronomical Society, and the editors of Astronomy & Astrophysics are thanked for granting permission to use previously published figures in this review.

References

Anders, E., & Grevesse, N. 1989, Geochim. Cosmochim. Acta, 53, 197
Antonucci, E., Gabriel, A. H., & Dennis, B. R. 1984, ApJ, 287, 917
Arge, C. N., & Mullan, D. J. 1998 Sol. Phys, 182, 293
Argiroffi, C., Maggio, A., & Peres, G. 2003, A&A, 404, 1033
Argiroffi, C., Drake, J. J., Maggio, A., et al. 2004, ApJ, 698, 925
Arzner, K., & Güdel, M. 2004, ApJ, 602, 363
Audard, M. 2003, Adv. Space Res., 32, 927
Audard, M., Behar, E., Güdel, M., et al. 2001b, A&A, 365, L329
Audard, M., Donisan, J. R., & Güdel, M. 2005, these proceedings
Audard, M., Güdel, M., Drake, J. J., & Kashyap, V. L. 2000, ApJ, 541, 396
Audard, M., Güdel, M., & Mewe, R. 2001a, A&A, 365, L318
Audard, M., Güdel, M., Sres, A., et al. 2003, A&A, 398, 1137
Audard, M., Telleschi, A., Güdel, M., et al. 2004, ApJ, in press
Ayres, T. R., Brown, A., Osten, R. A., et al. 2001, ApJ, 549, 554
Brickhouse, N. S., Dupree, A. K., & Young, P. R. 2001, ApJ, 562, L75
Brinkman, A. C., Behar, E., Güdel, M., et al. 2001, A&A, 365, L324
Chung, S. M., Drake, J. J., Kashyap, V. L., et al. 2004, ApJ, 606, 1184
Craig, I. J. D., & Brown, J. C., 1976a, Nature, 264, 340
Craig, I. J. D., & Brown, J. C., 1976b, A&A, 49, 239
Dennis, B. R., & Zarro, D. M. 1993, Sol. Phys., 146, 177
Dere, K. P., Bartoe, J.-D. F., & Brueckner, G. E. 1989, Sol. Phys., 123, 41
Drake, J. J. 2003, ApJ, 594, 496
Drake, J. J., & Sarna, M. J. 2003, ApJ, 594, L55
Drake, J. J., Brickhouse, N. S., Kashyap, V., et al. 2001, ApJ, 548, L81
Drake, J. J., Laming, J. M., & Widing, K. G. 1995, ApJ, 43, 393
Drake, J. J., Laming, J. M., & Widing, K. G. 1997, 478, 403
Drake, S. A. 1996, ASP Conf. Ser. 99: Cosmic Abundances, 215
Favata, F., & Micela, G. 2003, Space Sci. Rev., 108, 577
Favata, F., & Schmitt, J. H. M. M. 1999, A&A, 350, 900
Feldman, U. & Laming, J. M. 2000, Phys. Scr., 61, 222
Fisher, G. H., Canfield, R. C., & McClymont, A. N. 1985, ApJ, 289, 425
Garcia-Alvarez, D., Drake, J. J., & Lin, L. 2005, these proceedings
Gondoin, P. 2003a, A&A, 400, 249
Gondoin, P. 2003b, A&A, 404, 355
Gondoin, P. 2004, A&A, 415, 1113
Gondoin, P., Erd, C., & Lumb, D. 2002, A&A, 383, 919
Grevesse, N., & Sauval, A. J. 1998, Space Sci. Rev., 85, 161
Güdel, M. 1997, ApJ, 480, L121
Güdel, M., 2004, A&A Rev., 12, 71
Güdel, M., Arzner, K., Audard, M., & Mewe, R. 2003b, A&A, 403, 115
Güdel, M., Audard, M., Briggs, K. R., et al. 2001a, A&A, 365, L336
Güdel, M., Audard, M., Kashyap, V. L., et al. 2003a, ApJ, 582, 423
Güdel, M., Audard, M., Magee, H., et al. 2001b, A&A, 365, L344
Güdel, M., Audard, M., Reale, F., et al. 2004, A&A, 416, 713
Güdel, M., Audard, M., Skinner, S. L., & Horvath, M. I. 2002c, ApJ, 580, L73
Güdel, M., Audard, M., Smith, K. W., et al. 2002b, ApJ, 577, 371
Güdel, M., Audard, M., Sres, A., et al. 2002a, in 35$^{\rm th}$ ESLAB Symposium, ASP Conf. Ser. 277, eds. F. Favata & J. J. Drake (San Francisco: ASP), 497
Güdel, M., Linsky, J. L., Brown, A., & Nagase, F. 1999, ApJ, 511, 405
Güdel, M., Telleschi, A., Skinner, S. L., et al. 2005, these proceedings
Hénoux, J.-C. 1995, Adv. Space Res., 15, 23
Hénoux, J.-C. 1998, Space Sci. Rev., 85, 215
Huenemoerder, D. P., Canizares, C., Drake, J. J., et al. 2003 ApJ, 595, 1131
Huenemoerder, D. P., Canizares, C., & Schulz, N. S. 2001, ApJ, 559, 1135
Kashyap, V. L., Drake, J. J., Güdel, M., & Audard, M. 2002, ApJ, 580, 1118
Laming, J. M. ApJ, in press
Laming, J. M., & Drake, J. J., 1999, ApJ, 516, 324
Laming, J. M., Drake, J. J., & Widing, K. 1995, ApJ, 443, 416

Linsky, J. L. 1985, Sol. Phys., 100, 333
Linsky, J. L. 2003, Adv. Space Res., 32, 917
Maggio, A., Drake, J. J., Kashyap, V., et al. 2004, ApJ, in press
McKenzie, J. F. 2000, Sol. Phys., 196, 329
Ness, J.-U. 2005, these proceedings
Neupert, W. M. 1968, ApJ, 153, L59
Osten, R. A., Ayres, T. R., Brown, A., et al. 2003a, ApJ, 582, 1073
Osten, R. A., Brown, A., Ayres, T. R., et al. 2000, ApJ, 544, 953
Osten, R. A., Hawley, S. L., Brown, A., et al. 2003b, IAU Symposium 219, 207
Parker, E. N. 1988, ApJ, 330, 474
Raassen, A. J. J., Mewe, R., Audard, M., et al. 2002, A&A, 389, 228
Raassen, A. J. J., Mewe, R., Audard, M., & Güdel, M. 2003b, A&A, 411, 509
Raassen, A. J. J., Ness, J.-U., Mewe, R., et al. 2003a, A&A, 400, 671
Reale, F., Güdel, M., Peres, G., & Audard, M. 2004, A&A, 416, 733
Sanz-Forcada, J., Favata, F., & Micela, G. 2004, A&A, 416, 281
Sanz-Forcada, J., Maggio, A., & Micela, G. 2003, A&A, 408, 1087
Scelsi, L., Maggio, A., Peres, G., & Gondoin, P. 2004, A&A, 413, 643
Schmitt, J. H. M. M., & Favata, F. 1999, Nature, 401, 44
Schmitt, J. H. M. M., & Ness, J.-U. 2002, A&A, 388, L13
Schmitt, J. H. M. M., & Ness, J.-U. 2004, A&A, 415, 1099
Schmitt, J. H. M. M., Ness, J.-U., & Franco, G. 2003, A&A, 412, 849
Schmitt, J. H. M. M., Stern, R. A., Drake, J. J., & Kürster, M. 1996, ApJ, 464, 898
Schwadron, N. A., Fisk, L. A., & Zurbuchen, T. H. 1999, ApJ, 521, 859
Smith, K. W., Güdel, M., & Audard, M. 2005, these proceedings
Stelzer, B., Burwitz, V., Audard, M., et al. 2002, A&A, 392, 585
Telleschi, A., Güdel, M., Briggs, K., et al. 2005, these proceedings
van den Besselaar, E., Raassen, A. J. J., Mewe, R., et al. 2003, A&A, 411, 587